CGU HS Committee on River Ice Processes and the Environment
14th Workshop on the Hydraulics of Ice Covered Rivers
Quebec City, June 20 - 23, 2007

Experimental Investigation of the Pressure Distribution beneath a Floating Ice Block

Karen E. Dow, Faye Hicks and Peter Steffler
Department of Civil and Environmental Engineering
University of Alberta, Edmonton AB, T6G 2W2
kdow@ualberta.ca ; faye.hicks@ualberta.ca ; peter.steffler@ualberta.ca

It is known that discrete ice floes approaching an ice cover from upstream will contribute to the lengthening of the cover or will become entrained in the flow. The entrained floe could be deposited beneath the ice cover contributing to the thickness of the cover. In the case of an existing ice jam, it is possible that the entrained ice floes may be transported under the ice jam down past the toe and then propelled upwards, impacting the intact sold ice cover downstream. Such occurrences would have the potential to crack and weaken the cover, which might in turn result in the release of the ice jam. If true, specific knowledge of the hydrodynamic forces acting on individual ice floes will be an important component of any model which attempts to predict the occurrence of ice jam release events.

Experimental studies were conducted in a re-circulating flume in the T. Blench Hydraulics Laboratory at the University of Alberta to increase the knowledge of the physical behaviour of ice floes in water, and the hydrodynamic forces that act on them. To achieve this, a hollow Plexiglas ice block outfitted with pressure taps, was constructed to facilitate measurements of the pressure distribution beneath an ice block. The dynamic pressure was measured under the block for various block thickness to depth ratios and flow velocities. The ice block stability was then evaluated from the pressure measurements by conducting a moment analysis. The results of the experimental study provided essential validation data for a numerical model to be used to further understand this problem.

1.0 Introduction

The transport and accumulation of ice is one of the more complicated problems in river ice hydraulics, because of the complex fluid dynamics surrounding individual ice floes. It is of relevance to the physics of ice cover development and ice jam formation, but is of particular in the context of ice jam release. Jasek (2003) notes that when large ice floes are transported downstream under an ice jam past its toe, then it is likely that these floes will be propelled upwards, impacting the underside of the intact solid ice cover. He suggests that such occurrences have the potential to crack and weaken the restraining ice cover, initiating the open leads which are believed to play an important role in the occurrence of ice jam release (Jasek, 2003). If true, specific knowledge of the hydrodynamic forces acting on individual ice floes will be an important component of any model which attempts to predict the occurrence of ice jam release events.

In the practical context of this problem, there are a number of component phenomena to consider. For example, the initial question is whether or not discrete ice floes approaching an ice jam accumulation from upstream will contribute to lengthening, or will be entrained in the flow and transported beneath the ice jam. For the latter case, the further question is whether or not the entrained floe will be transported all the way past the ice jam toe, to be in a position to rise under the intact restraining ice cover.

At present, much of our knowledge of these processes is necessarily qualitative, due to the inherent logistical difficulties and safety issues which arise when trying to measure dynamic ice processes in the field. This is particularly difficult for ice floe transport under ice jams. As a consequence, we must rely in large part on experimental and numerical work to further understand the mechanics of ice floe entrainment and transport, and that is the purpose of this investigation. Here we discuss some preliminary results of the first phase of this experimental investigation, in which we focus on the issue of ice floe entrainment at the leading edge. Current theory and observations (e.g. Beltaos, 1995) suggest that the leading edge of an ice jam accumulation behaves as a narrow jam, with floe entrainment or juxtapositioning being the dominant local processes. Healy and Hicks (2001) observed this same tendency near the leading edge of ice jams forming in a laboratory flume.

Numerous studies have already been conducted to examine this problem of ice block stability. Early investigations of this phenomenon focused on defining the critical approach velocity or critical densimetric Froude number (based on approach flow velocity and block thickness) at which floating ice blocks at the leading edges of intact ice covers are submerged (Pariset and Hausser, 1961; Ashton, 1974; Uzuner and Kennedy, 1972; Larsen, 1975). Daly and Axelson (1990) examined the problem analytically and determined that instability was reached when the underturning moment exceeded the righting moment. Coutermarsh and McGilvary (1991, 1993, 1994) attempted to measure the two dimensional pressure distribution along the bottom surface of a floating block and found both positive (stabilizing) and negative (destabilizing) pressures acted on the block, with a characteristic saddle shape in the pressure distribution. They observed that changes in flow velocity had little effect on the pressure distribution but primarily changed the pressure magnitude. More recently Hara *et al.* (1996) and Kawai *et al.* (1997) conducted a

series of experiments investigating the movement of ice floes at the edge of an ice cover characterizing the movement and the critical densimetric Froude number at movement. They focused on the shape of the edge of the ice cover and the thickness of the ice block.

With recent advances in numerical and experimental technology that allow for better flow visualization and determination, more information about the mechanics of the problem can now be now realized. The objective of this phase of our study is to examine the steady state stability of floating ice blocks that have come to rest against an intact ice cover using by measuring the pressure distribution beneath a floating ice block. We seek to increase our knowledge of the stability behaviour of floating ice floes and the hydrodynamic forces that act upon them. Ultimately, the results of this study will be used to validate a 3-D numerical model which can then be used to investigate a broad range of scenarios. The intent of this paper is to share some of the early experimental observations on the pressure reduction beneath a floating ice block.

2.0 Experimental Apparatus and Procedures

The experiments were carried out in the 7.5 m (metre) long re-circulating flume located in the T. Blench Hydraulics Lab at the University of Alberta. This rectangular flume, pictured in Figure 1, has 0.45 m high side walls and a width of 0.75 m. The bed and walls are made of glass to facilitate modern optical measurement techniques, such as particle image velocimetry (which will be employed in phase 2 of the study). The pump is controlled by a variable frequency drive and has a maximum discharge of 150 L/s. Flow rates are measured with a magnetic flow meter.

A hollow rectangular block 50 cm long, 75 cm wide and total thickness of 10.16 cm was constructed of Plexiglas. To enable the simulation of various thicknesses of floating ice, the block was held in position by four threaded rods that allowed for height adjustment, as shown in Figure 2. Approach flow velocity profiles were measured using a micro-ADV (acoustic Doppler velocimeter). In order to measure the pressure distribution beneath the block, it was outfitted with 20 pressure taps at various positions along its centerline, each connected to a manometer board using ¼" O.D. Tygon tubing. The pressure tap locations are summarized in Table 1 and shown in Figure 3.

Table 1. Pressure tap locations, y = 0 cm is the centerline of the block.

#	*x* (cm)	*y* (cm)	#	*x* (cm)	*y* (cm)
1	1.25	0	11	5.0	-1.25
2	1.5	1.25	12	6.5	0
3	1.75	2.5	13	8.0	0
4	2.0	-1.25	14	10	0
5	2.25	-2.5	15	12.5	0
6	2.5	0	16	15	0
7	3.0	1.25	17	20	0
8	3.5	-1.25	18	25	0
9	4.0	0	19	35	0
10	4.5	1.25	20	45	0

The block was positioned in the flume with the leading edge at x = 4 m, so as to ensure the flow would be fully developed before reaching the block, and also to ensure it would not be affected by the outlet. The block was positioned vertically by adjusting the threaded rods to the desired elevation and using a digital level to ensure the block was level. The effective thickness of the "ice" was determined based upon assuming a typical specific gravity of ice of 0.92. The water depth and block height were measured using a point gauge.

De-mineralized water was de-aired for use in the manometer tubing to minimize the air in the lines. Once the block was positioned, the tubing was flushed to eliminate any air bubbles. To accomplish this, a Nalgene container was raised to the ceiling of the lab, creating sufficient head to flush the tubing effectively.

Three different ice thicknesses were tested at three different flow rates for a total of nine tests total, as summarized in Table 2. Here t refers to the ice thickness, H the approach flow depth, Q the flow rate, V the approach average velocity, H_u the flow depth under the ice block, V_u the average velocity beneath the ice block, $\boldsymbol{F}_a$ is the Froude number of the approach flow, $\boldsymbol{F}_u$ is the Froude number of the flow under the block, and $\boldsymbol{R}_a$ is the Reynolds number of the approach flow. In each case, the manometer board was tilted to 30° to allow for more accurate readings. A digital camera on a tripod was set up above the manometer board and a photograph was taken with the flume flow at rest, in order to obtain the initial reading for each tube. The flow was increased to the desired flow rate and allowed to stabilize for five minutes. Three photographs were then taken of the manometer board to document the ultimate steady state conditions (Figure 4). The dynamic pressures were then calculated using the differences in manometer levels measured before the flow was initiated and after the levels had stabilized. Each test was repeated twice.

Table 2. Summary of data for the nine tests.

Run #	t (cm)	H (cm)	Q (L/s)	t/H	V (cm/s)	V_u (cm/s)	$\boldsymbol{F}_a$	$\boldsymbol{F}_u$	$\boldsymbol{R}_a$
1	3.35	30.2	79	0.11	35.0	38.9	0.20	0.24	1.06E+05
2	3.35	30.2	111	0.11	49.0	54.5	0.28	0.33	1.48E+05
3	3.35	30.2	142	0.11	62.7	69.9	0.36	0.43	1.89E+05
4	6.02	30.03	79	0.20	35.2	43.2	0.21	0.28	1.06E+05
5	6.02	30.03	111	0.20	49.2	60.4	0.29	0.39	1.48E+05
6	6.02	30.03	142	0.20	63.1	77.4	0.37	0.50	1.90E+05
7	8.39	29.02	79	0.29	36.5	49.7	0.22	0.34	1.06E+05
8	8.39	29.02	111	0.29	51.0	69.5	0.30	0.48	1.48E+05
9	8.39	29.02	142	0.29	65.3	89.0	0.39	0.62	1.90E+05

3.0 Results and Discussion

The dynamic pressures measured for each case is shown in Figures 5 through 7. The pressure shown is the average of the two repeats. In general the shape of the pressure distribution was found to be consistent for all cases, exhibiting an initial pressure drop at the leading edge of the ice block that persists for a certain distance from the leading edge, before decreasing gradually to a second (lower) plateau. In each of the three cases, the pressures decreased as the flow rate increased, reflecting the increasing flow acceleration beneath the block. Also, comparing the three cases, it is evident that as the thickness of the block increases (i.e. as the *t/H* ratio increases), the pressures beneath the block decrease. A greater thickness of ice produces a larger obstruction to the flow and consequently a larger velocity beneath the ice block. Also as the ice thickness increases, the length of the initial pressure drop region increases, as well as the overall length of recovery to the final pressure plateau. This can be attributed to the size of the separation recirculation zone at the leading edge of the ice block, which appears to increase with ice thickness.

It would be useful to combine these results into a non-dimensional form and it appears from the consistent shape of the pressure distributions that this should be possible. This can be achieved by employing a coefficient of the form:

$$C = \frac{P}{\frac{1}{2}\rho V^2} \qquad [1]$$

where P is a pressure and V is a velocity. To examine this in terms of an overall coefficient, P would be the average pressure across the block and V would be the average velocity.

In order to non-dimensionalize the pressure distributions, the pressure at each measurement location can be converted into a coefficient by using the above equation along with the under ice average velocity. To non-dimensionalize the length scale, we can define:

$$\xi = \frac{x}{t_s} \qquad [2]$$

where x is the distance from the leading edge of the ice block and t_s is the submerged thickness of the ice block. We define three more variables in order to present the non-dimensional results. ξ_{50} is defined as:

$$\xi_{50} = \frac{x_{50}}{t_s} \qquad [3]$$

where x_{50} is the location at which the pressure is midway between the initial and final pressure plateau values. $C_{\min}$ is the minimum value of the sink coefficient, C, calculated for each test case,

or in other words the value of C for the initial pressure plateau. $C_{asymptote}$ is the value of C at the final pressure plateau near the end of the block. For the first cases, t/H = 0.1 this is straight forward as the data captures both the initial and final pressure plateaus. For t/H = 0.2 and t/H = 0.3, only the initial plateau was captured from the data. However the final plateau values for these two cases, which can be referred to as the venturi pressure, can be approximated using the Bernoulli equation. The calculated values for these two cases, as well as the values measured from the first case, are summarized in the table below. In this table t_s refers to the submerged block thickness, $P_{asymptote}$ refers to the final pressure plateau, and $\boldsymbol{R}_b$ is the Reynolds number using the block submerged thickness and the under block velocity.

Table 3. Summary of data used for non-dimensionalization.

Run #	t_s (cm)	$\boldsymbol{R}_b$	$P_{asymptote}$ (Pa)	x_{50} (cm)
1	3.08	1.20E+04	-22.65	5.25
2	3.08	1.68E+04	-44.6	12.5
3	3.08	2.15E+04	-71.99	18
4	5.54	2.39E+04	-31.19	25
5	5.54	3.34E+04	-60.99	26.5
6	5.54	4.29E+04	-100.32	28
7	7.72	3.84E+04	-56.96	31
8	7.72	5.36E+04	-111.4	29
9	7.72	6.87E+04	-182.75	27.5

Figure 8 shows the non-dimensional data presented as a ratio of $\frac{C - C_{asymptote}}{C_{\min} - C_{asymptote}}$ versus a ratio of ξ/ξ_{50}. The data is presented in this manner to remove the constant venturi pressure, due to the flow constriction that is present in each test, in order to bring all the curves to zero. When this is done the pressure reduction due to the effect of the separation zone remains. It is evident that the data from the nine tests collapse together rather well. This figure provides the general shape of the pressure distribution beneath a floating ice block which is useful in predicting the pressure distribution beneath an ice block. In order to use this figure as a predictive tool for the pressure distribution, relationships for x_{50} and C_{min} are needed.

Figure 9 shows a relationship for x_{50}, plotted as x_{50}/H versus t_s/H. From this figure it is evident that, in general, as the submerged thickness increases, the midpoint of the pressure drop due to the leading edge effect, x_{50}, is shifted further along the block. Comparing Runs 1 through 3 it is clear that x_{50} increases with increasing discharge, so as the velocity increases the pressure distribution due to leading edge effects lengthens. A similar trend is seen for Runs 4 through 6.

Runs 7 through 9 exhibit the opposite effect; however, the difference could be due to data scatter and one could say the curves would become asymptotic at a x_{50}/H of 1.0 for cases where the submerged thickness is greater than 20% of the approach flow depth.

Figure 10 shows a relationship for $C_{\min} - C_{asymptote}$ based on the Reynolds number calculated using the submerged block thickness and under block average velocity, $\boldsymbol{R_b}$. $C_{asymptote}$ can be calculated using the Bernoulli equation for any case. The results are remarkably constant with the majority of the runs at a value of approximately -0.7. Run 3 could be considered as an outlier while Run 1 may be considered in a transition zone; however, it should be noted that the measured pressure differences for Run 1 were very close to the minimum resolution level of the apparatus. The constant value of -0.7 suggests that the difference between the minimum pressure and the venturi pressure is based solely on the under block velocity.

5.0 Summary & Future Work

Preliminary results of an experimental study on the steady state pressure distribution under floating ice blocks have been presented. This knowledge of the hydrodynamic forces that act on individual ice floes is crucial to the prediction of ice jam release events as much of the current knowledge of these processes is necessarily qualitative. In order to examine the stability of floating ice blocks the dynamic pressure distribution beneath a model ice block was measured for nine different test cases. The pressure was shown to decrease for increasing submerged thickness to flow depth ratios as well as for increasing velocity. The pressure distribution was non-dimensionalized to show that the data from all nine cases collapses rather well to a form that could be used to predict a pressure distribution beneath a floating ice block. More data is necessary to fill in the gaps and get a complete picture of the relationships, however this data shows promise.

The next stage of this experimental study will be to examine the transverse pressure distribution across the block, for these same nine cases. This will give a complete picture of the pressure distribution across the entire bottom surface of the block. All experiments will then be repeated with different leading edge shapes. It is evident that the separation recirculation zone is important to the pressure distribution and, in turn, the stability of the ice block; therefore different leading edge shapes would be expected to affect this separation zone significantly.

The final stage of the experimental study will be to employ a particle image velocimetry (PIV) system to characterize the velocity field around an ice floe approaching an intact ice cover, and as it becomes entrained in the flow. The force and moment of the moving ice piece can then be inferred from its measured trajectory and the surrounding velocity field.

Finally, the results from the experimental study will be combined with an ongoing numerical study that uses a commercially available three dimensional computational fluid dynamics (CFD) package, ANSYS CFX to model the stability of a floating ice block under steady flow conditions.

Acknowledgments

This research is supported by scholarships to the first author from the Natural Sciences and Engineering Research Council of Canada (NSERC) and Alberta Ingenuity, and through NSERC research grants to the other two authors. This support is gratefully acknowledged. The authors also thank Perry Fedun and Chris Krath for their assistance in developing the experimental setup and Dr. Mark Loewen for his advice on these experiments.

References

Ashton, G.D., 1974. Froude criterion for ice-block stability. Journal of Glaciology, 13(68), pp. 307-313.

Beltaos, S. (1995). River Ice Jams. Water Resources Publications, LLC, Highlands Ranch, Colorado, 372 pp.

Coutermarsh, B. & McGilvary, W.R., 1991. Pressure distribution of an underturning ice floe. Proc. 6th Workshop on River Ice, pp. 143-163.

Coutermarsh, B.A. and McGilvary, W.R., 1993. Static analysis of floating ice block stability. Journal of Hydraulic Research, 31(2), pp. 147-160.

Coutermarsh, B and McGilvary, R., 1994. Analyzing the stability of floating ice floes. CRREL Report 94-13, 19 pp.

Daly, S.F. and Axelson, K.D., 1990. Stability of floating and submerged blocks. Journal of Hydraulic Research, 28(6), pp. 737-752.

Hara, F., Kawai, T., Hanada, M., Nishihata, A., and Saeki, H., 1996. Movement of ice blocks under an ice cover. Proceedings of IAHR Ice Symposium, Beijing, pp. 769-778.

Healy, D. and Hicks, F. (2001) "Experimental Study of Ice Jam Shoving" Proc. 11th Workshop on River Ice, Ottawa, May, pp. 126-144.

Jasek, M., 2003. Ice jam release and break-up front propagation. Proceedings of the 12th workshop on the hydraulics of ice covered rivers, The CGU HS Committee on River Ice Processes and the Environment. June 19-20, 2003, Edmonton, AB, pp. 348-368.

Kawai, T., Hara, F., Masaki, S., Nishihata, A., and Saeki, H., 1997. Experimental study on the process of ice jam development. Proceedings of 9th CRIPE, pp. 245-256.

Larsen, P., 1975. Notes on the stability of floating ice blocks. Proceedings of the IAHR third international symposium on ice problems. Hanover, NH, IAHR, pp. 305-313.

Pariset, E. and Hausser, R., 1961. Formation and evolution of ice covers on rivers. Transactions of the Engineering Institute of Canada, 5(1), pp. 41-49.

Uzuner, M.S. and Kennedy, J.F., 1972. Stability of floating ice blocks. Journal of the Hydraulics Division, 98 (HY12), pp. 2117-2133.

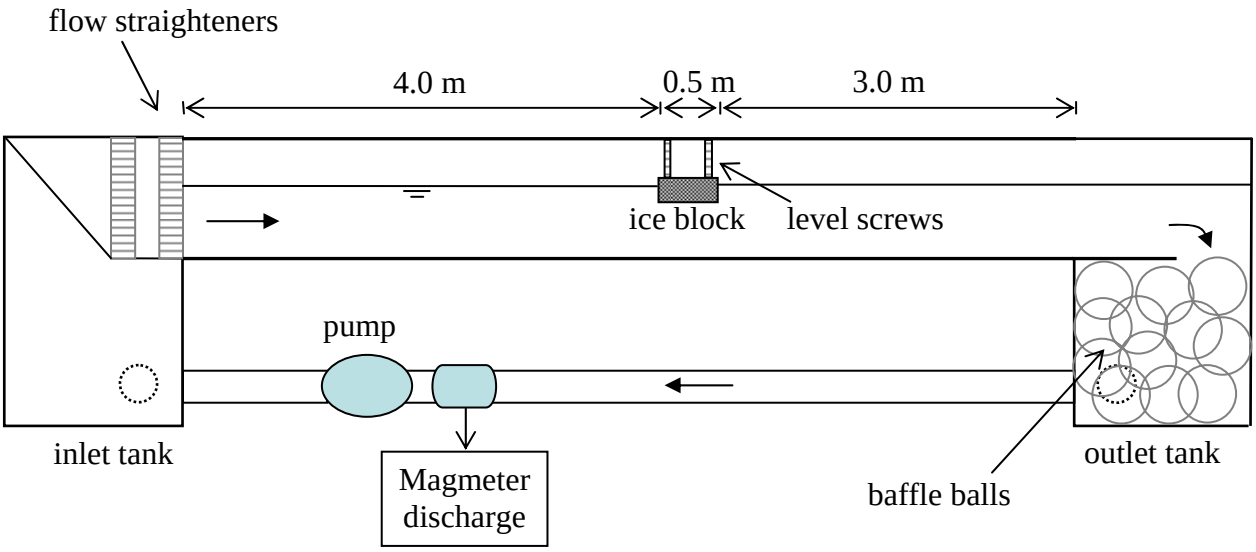

Figure 1. Experimental setup schematic.

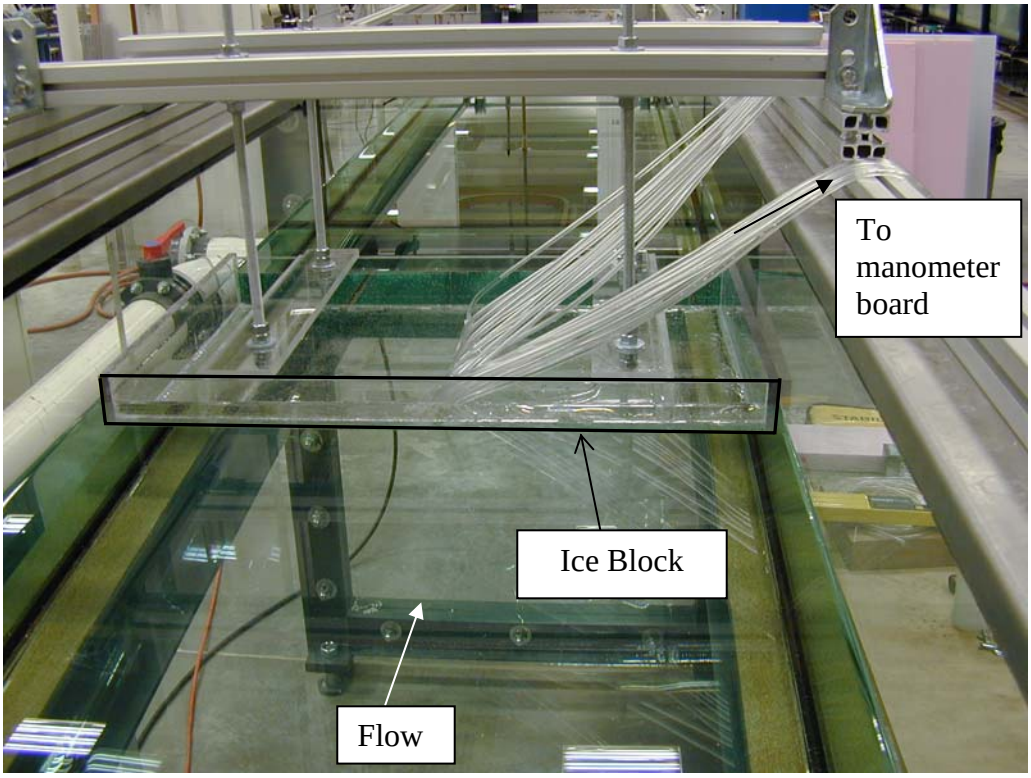

Figure 2. Experimental flume - Ice block setup, looking downstream.

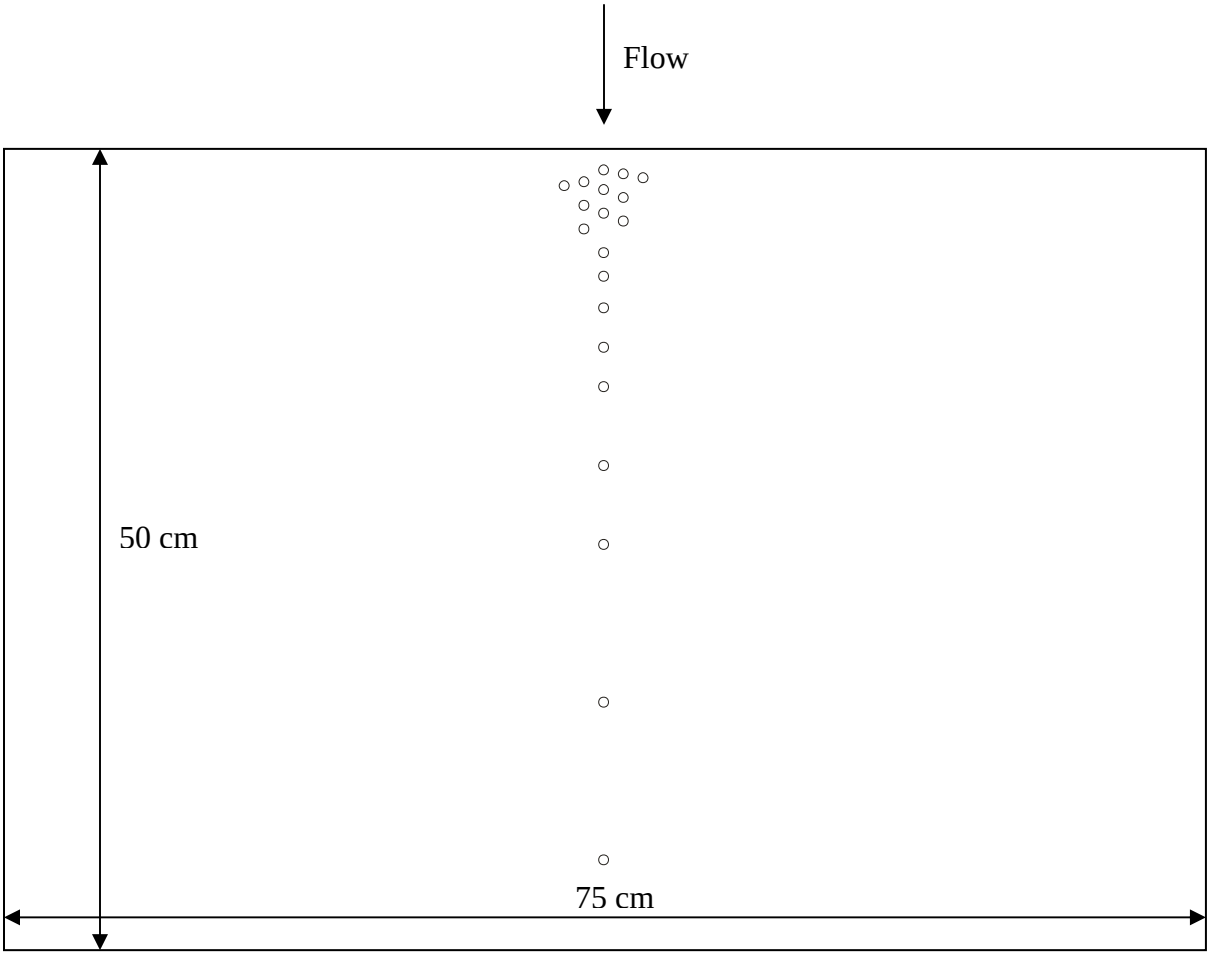

Figure 3. Locations of pressure taps in ice block.

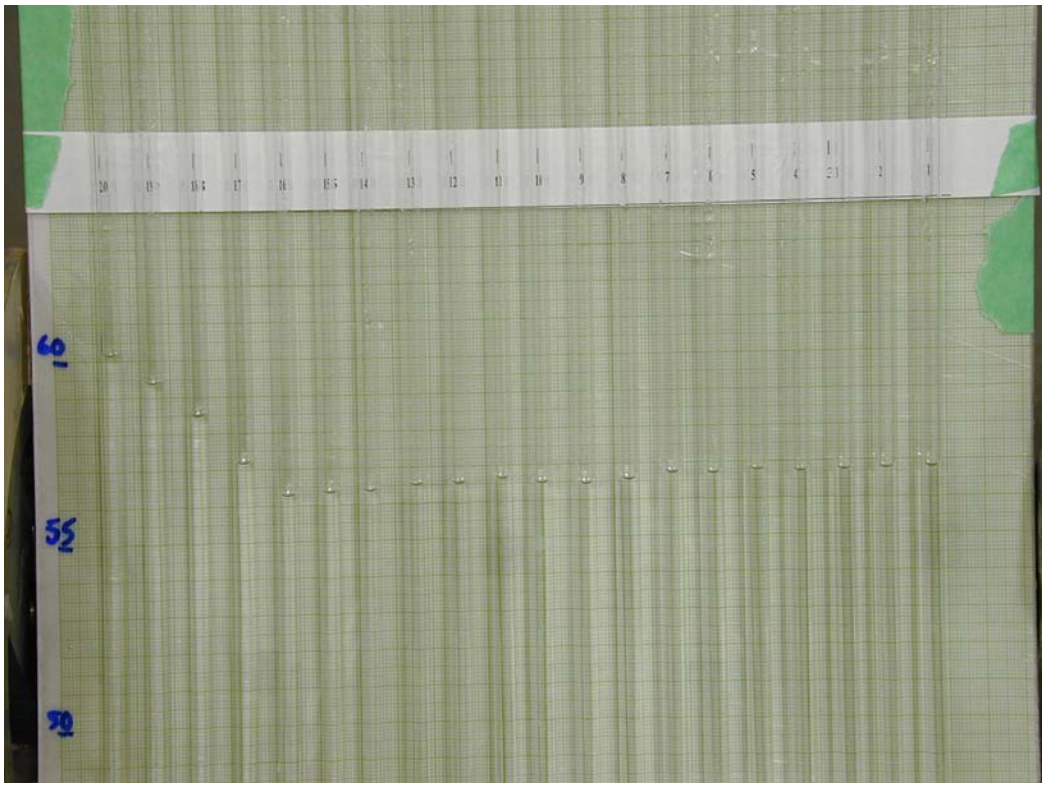

Figure 4. Manometer board for Q = 111 L/s and t/H = 0.2.

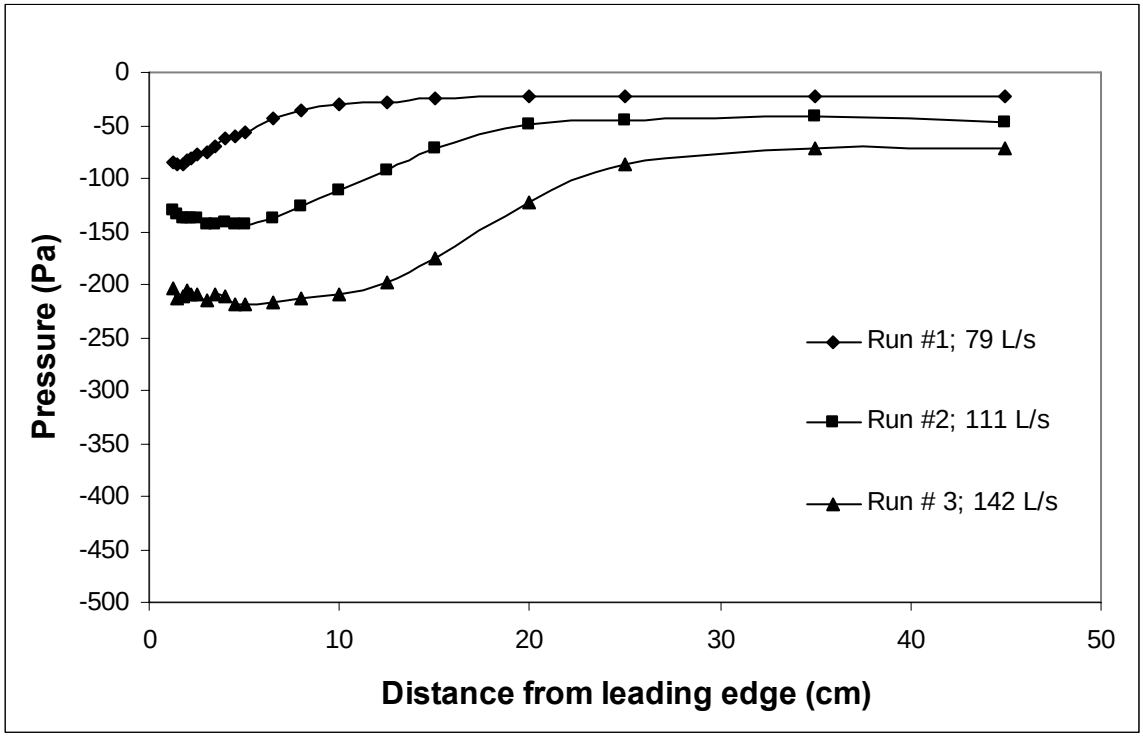

Figure 5. Dynamic pressures measured under the ice block for t = 3.35 cm, H = 30.2 cm (t/H = 0.11).

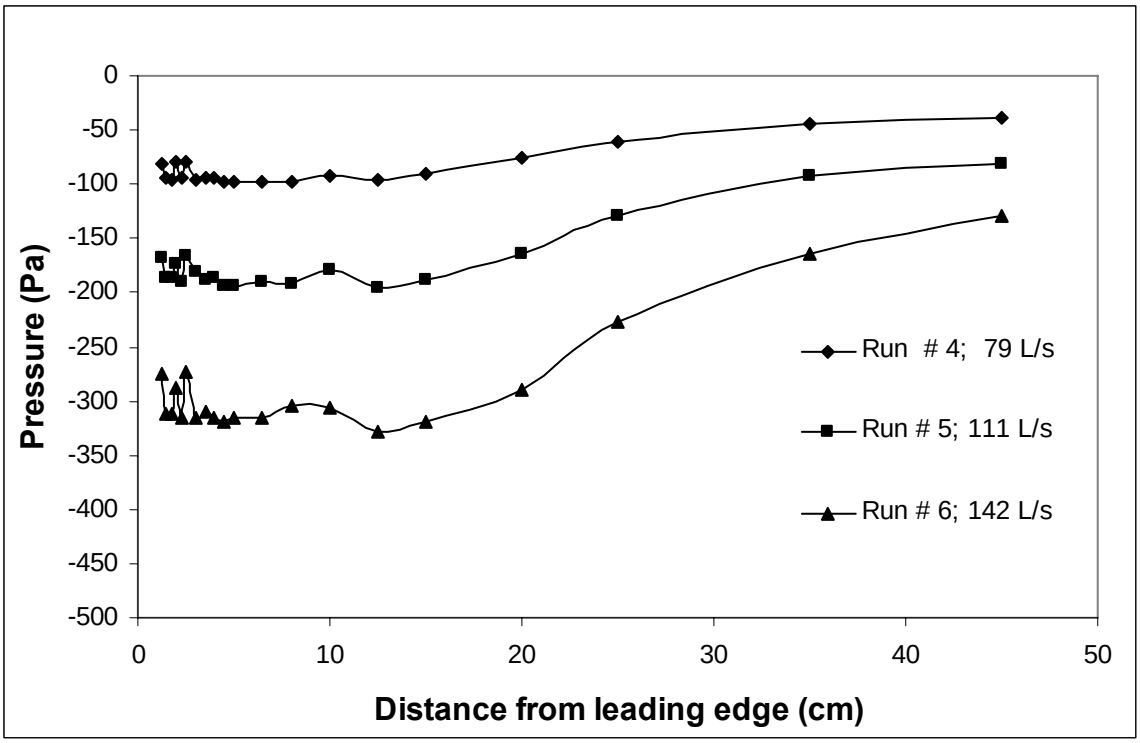

Figure 6. Dynamic pressures measured under the ice block for t = 6.02 cm, H = 30.03 cm (t/H = 0.20).

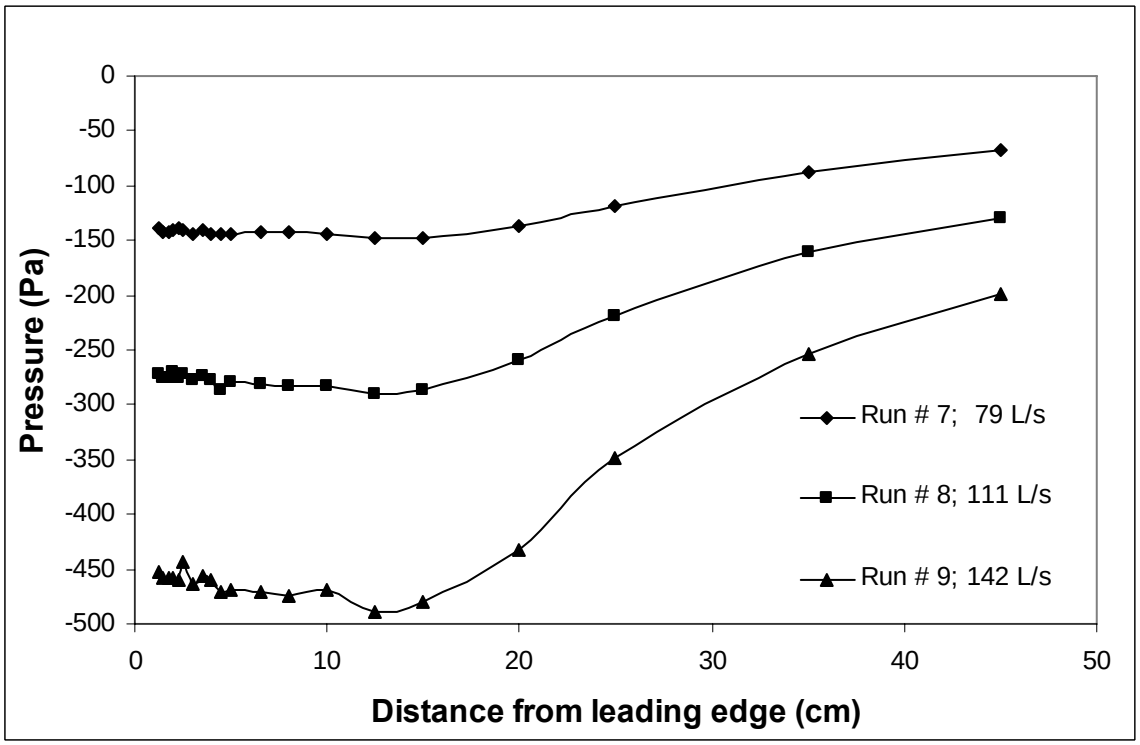

Figure 7. Dynamic pressures measured under the ice block for t = 8.39 cm, H = 29.02 cm (t/H = 0.29).

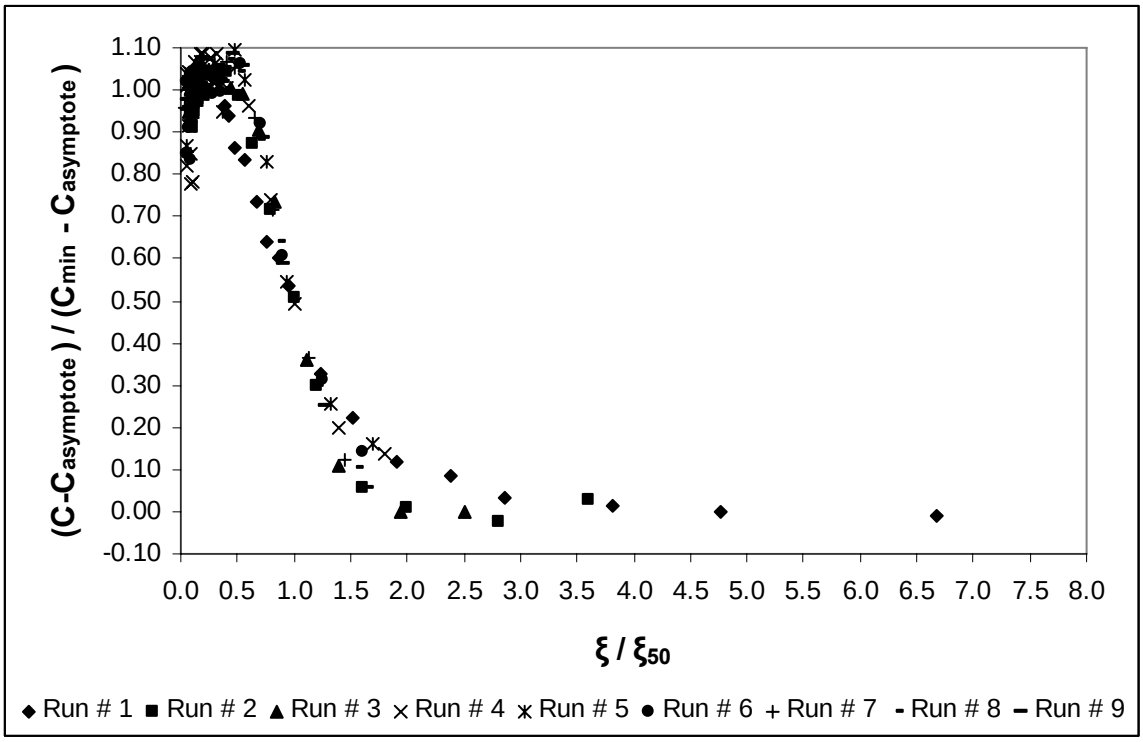

Figure 8: Non-dimensionalized data from all test cases.

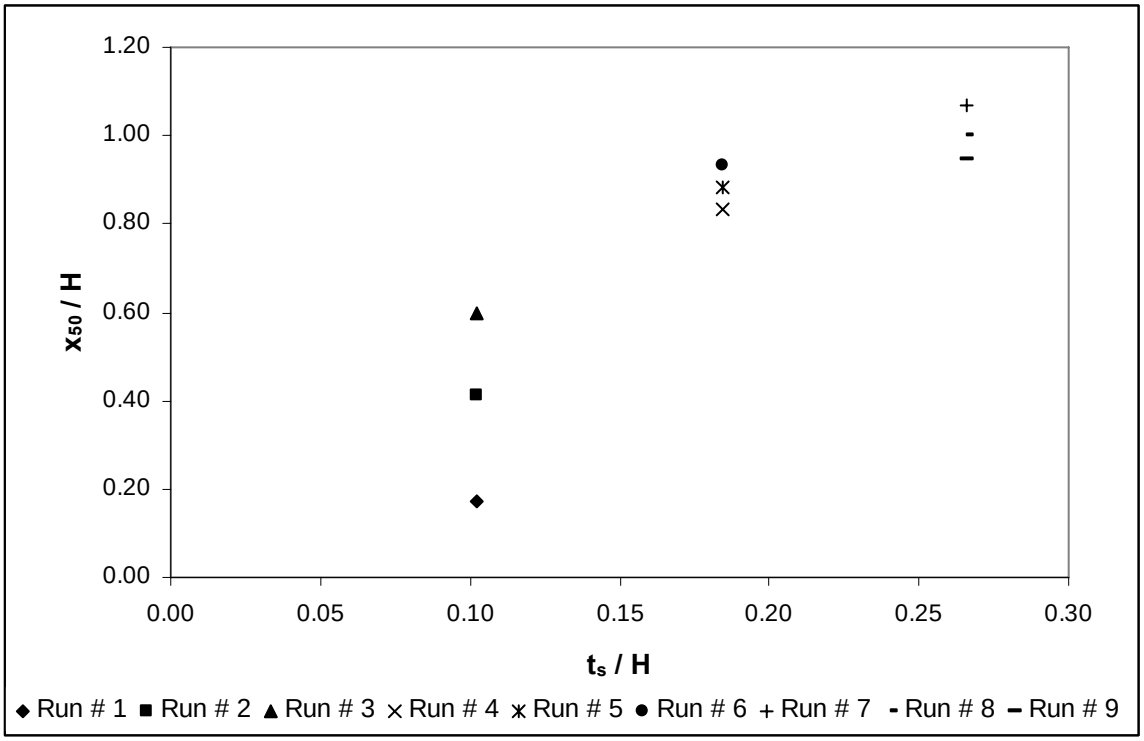

Figure 9. Non-dimensional relationship to determine x_{50}.

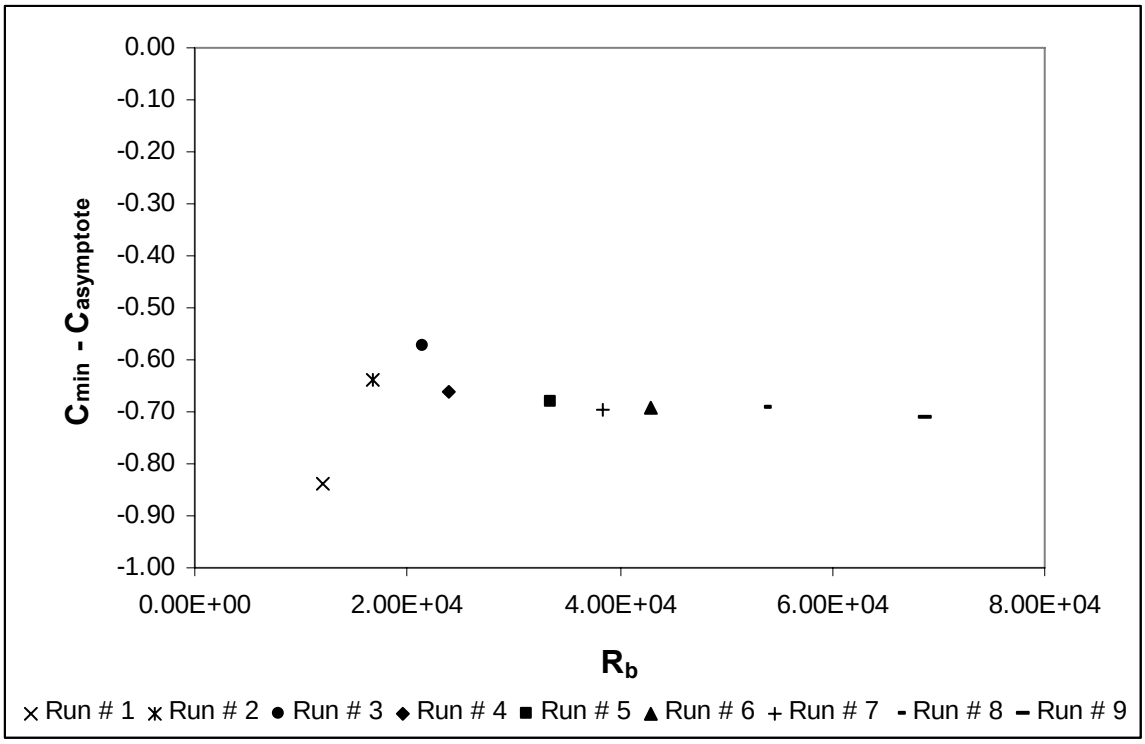

Figure 10. Non-dimensional relationship to determine C_{min}.